NeuroImage 204 (2020) 116212

Contents lists available at ScienceDirect

NeuroImage

journal homepage: www.elsevier.com/locate/neuroimage

Neural correlates of enhanced response inhibition in the aftermath of stress

Jingjing Chang [a], Jianping Hu [b], Chiang-Shan R. Li [c,d], Rongjun Yu [e,*]

[a] Guangdong Key Laboratory of Mental Health and Cognitive Science, Center for Studies of Psychological Application, School of Psychology, South China Normal University, Guangzhou, China
[b] Laboratory for Behavioral and Regional Finance, Guangdong University of Finance, Guangzhou, China
[c] Department of Psychiatry, Yale University School of Medicine, New Haven, CT, USA
[d] Department of Neuroscience, Yale University School of Medicine, New Haven, CT, USA
[e] Department of Psychology, National University of Singapore, Singapore

ARTICLE INFO

Keywords:
Stress
Stop signal task
Response inhibition
Striatum
Prefrontal cortex

ABSTRACT

Life stress has been shown to impact cognitive functions, including inhibitory control. However, the immediate effects of acute stress on inhibitory control and the underlying neural mechanisms remain unclear. In a behavioral pilot study (N = 30) and a within-subject functional magnetic resonance imaging study (N = 30), we examined how acute stress induced by Trier Social Stress Test influenced inhibitory control in a stop signal task. Behavioral results across two studies showed that stress consistently improved inhibitory control. Shorter stop signal reaction time (SSRT) in stress as compared with control condition was associated with stronger connectivity between the superior/middle frontal gyrus (SFG/MFG) and striatum. Dynamic causal modeling revealed distinct best models under stress and control condition, with an enhanced interaction between the SFG/MFG and the striatum after stress exposure. This research identified the SFG/MFG-striatum network as a key circuit underlying acute stress-elicited enhancement of inhibitory control in a stop signal task.

1. Introduction

Stress is widespread in daily life and can be induced by various stressors, ranging from small events, such as choosing a restaurant for lunch, to bigger events, like the death of a loved one. Both acute and chronic stress affect several brain regions, including the prefrontal cortex, hippocampus, amygdala and striatum (Chang and Yu, 2018a, 2018b; McEwen et al., 2015; Ulrich-Lai and Herman, 2009). For example, exposure to a chronic stressor leads to morphological changes of the prefrontal cortex (PFC), e.g., a significant decrease of dendrites, as well as impaired PFC dependent cognitive functions (Liston et al., 2006; Wellman, 2001). The striatum plays an important role in various functions, like reward processing, response inhibition, and learning. Both human and rodent studies have shown that the striatum-based habitual system takes over the learning process after stress, suggesting the sensitivity of striatum cortex to stress (Quirarte et al., 2009; Schwabe and Wolf, 2012). Taken together, accumulating evidence suggests that stress has a profound impact on the fronto-striatal network and related cognitive functions (Schwabe, 2013; Shields et al., 2016a,b; Yu, 2016).

Response inhibition, the ability to stop an inappropriate action, is a core process of executive function (Diamond, 2013). The stop signal task (SST) is a useful paradigm to study response inhibition, in which a go signal might be followed by a stop signal to inhibit the have initiated response (Garrett and Maddock, 2001; Verbruggen and Logan, 2008). The response inhibition is measured by the length of time of the stop process (i.e., SSRT). The SSRT has been considered as the most suitable index for cognitive inhibition (Roos et al., 2017; Verbruggen and Logan, 2008). Previous studies in humans and animals have shown that chronic life stress impairs cognitive function, including response inhibition (Mika et al., 2012; Mueller et al., 2010). However, the immediate effects of acute stress on inhibitory control are far from clear. Using a stop signal task (SST) and a cold pressor test, Schwabe et al. found that acute stress promoted inhibitory responses and that stressor-enhanced cortisol level was negatively correlated with the stop signal reaction time (SSRT). Furthermore, individuals who received the mineralocorticoid receptors antagonist spironolactone did not demonstrate these effects (Schwabe et al., 2013). In addition, recent meta-analyses suggest that acute stress improved response inhibition (Shields et al., 2016a,b), especially 15–135 min after stress exposure (Shields et al., 2015). However, other studies have reported inconsonant results (McGrath et al., 2016; Roos et al., 2017; Scholz et al., 2009; Starcke et al., 2016). For example, a significant SSRT reduction was observed in the control group for

* Corresponding author. Department of Psychology, National University of Singapore, 117570, Singapore.
E-mail address: psyyr@nus.edu.sg (R. Yu).

https://doi.org/10.1016/j.neuroimage.2019.116212
Received 19 April 2019; Received in revised form 12 September 2019; Accepted 18 September 2019
Available online 20 September 2019
1053-8119/© 2019 Elsevier Inc. All rights reserved.

post-SST vs. pre-SST, while this significant task practice effect disappeared after Trier Social Stress Test (TSST), indicating the impairment of inhibitory control under stress (Roos et al., 2017). The discrepancy may result from differences in the characteristics of stressors (e.g., social or physical), the intensity of stressor, the cognitive tasks, the time interval between the stress manipulation and task, age and gender of the subject populations (Jiang and Rau, 2017; Mika et al., 2012; Shields et al., 2015; Shields et al., 2016a,b). In the present study, a within-subject design was adopted to mitigate the impact of individual differences. We used TSST (including both public speaking and mental arithmetic tasks) to induce acute social stress. The TSST is the gold standard and most commonly employed paradigm and has been shown to reliably elicit a high level of cortisol (McRae et al., 2006). Given that the cortisol reaches its peak level at about 30 min after stress manipulation (Schwabe et al., 2013; Schwabe et al., 2008), the time interval between the TSST and SST was about 30 min in our study.

Previous fMRI studies using the SST showed that the response inhibition was associated with the activation of brain regions in the frontal cortex and basal ganglia, including the inferior frontal gyrus, middle frontal gyrus, superior frontal gyrus, anterior cingulate cortex, pre-supplementary motor area, striatum and subthalamic nucleus (Aron et al., 2007; Aron and Poldrack, 2006; Li, Huang, Constable and Sinha, 2006; Sharp et al., 2010; Verbruggen and Logan, 2008). Specifically, successful response inhibition was related to greater activation of the right inferior frontal gyrus and pre-supplementary motor area, while unsuccessful inhibition was correlated with the activation in the anterior cingulate cortex (Aron et al., 2007; Sharp et al., 2010). Many lines of evidence have consistently implicated the fronto-striatal circuit in response inhibition (Bari and Robbins, 2013; Courtney et al., 2013). It is well known that the prefrontal cortex plays an important role in response selection and inhibition (Adler et al., 2010; Krivoshapkin et al., 2007). Evidence has also accumulated which supports striatal mechanisms in the inhibition process (Morein-Zamir and Robbins, 2015; Simmonds et al., 2008; Swann et al., 2012; Zandbelt and Vink, 2010). For instance, a previous study of the SST reported increased striatal activity during successful versus unsuccessful stopping (Zandbelt and Vink, 2010). In addition, caudate and putamen dopamine D_2/D_3 receptor availability was negatively correlated with the stop signal reaction time and positively correlated with inhibition-related activation in the frontostriatal circuitry, suggesting the important role of dorsal striatum during inhibition (Ghahremani et al., 2012). Furthermore, the connectivity between the PFC and striatum is also involved in stopping inappropriate actions, and the connectivity strength is related to the efficiency of response inhibition (Courtney et al., 2013; Duann et al., 2009; Jahfari et al., 2011; Zandbelt and Vink, 2010). A study using psychophysiological interaction found that during successful suppression of a response in the stop-signal anticipation task, the activity of striatum had a significantly positive correlation with the activity in the right inferior frontal cortex (Zandbelt and Vink, 2010). Given that the frontal and striatal cortex are vulnerable to stress and also play important roles in the inhibition process, the fronto-striatal circuits may represent an important target to investigate the effects of acute stress on response inhibition. Although focusing on the effect of chronic stress, a study showed that success change (vs. success go) trials, which engaged motor inhibition involved higher activation of the PFC and striatum in the early-life stress group as compared to the control group, suggesting the roles of frontostriatal circuitry in inhibition under chronic stress (Mueller et al., 2010).

In the present study, by combining the Trier Social Stress Test (TSST) and SST, we firstly conducted a pilot behavioral study to explore whether and how acute psychological social stress affected behavioral performance in response inhibition. Subsequently, an fMRI study was performed to replicate the behavioral findings and further examine the neural mechanisms underlying the impact. Specifically, based on recent meta-analyses (Shields et al., 2015; Shields et al., 2016a,b), we predicted that response inhibition could be improved after stress exposure, and the activation of the prefrontal cortex and striatum as well as prefrontal-striatal connectivity increased during successful stopping. Further, we employed dynamic causal modeling (DCM) to explore stress-elicited changes in directed connectivities of the PFC and striatum during response inhibition.

2. Methods and results

2.1. Experiment 1: a behavioral study

2.1.1. Participants

Thirty right-handed volunteers 21.2 ± 1.7 (mean $\pm$ SD; range 19–25) years of age, including 14 females, participated in this study. All participants were healthy and without a history of major medical, psychiatric, or neurological disease. None of them reported use of illicit substances or current use of any psychoactive medications. In addition, no female participants reported use of hormonal contraceptives. Participants were instructed to refrain from heavy exercise and caffeine for at least 12 h before the experiments. No participants had previously enrolled in stress-related research. All participants provided written informed consent according to a protocol approved by the South China Normal University Institutional Review Board.

2.1.2. Experimental design and procedure

In humans, the level of endogenous cortisol has been reported to be relatively stable and low in the afternoon (Deuschle et al., 1997). Following previous studies (Qin et al., 2012; Schwabe and Wolf, 2012), all experiments were conducted between 2 and 6 p.m. Participants were exposed to acute stress and control conditions with at least 30 days in between the two sessions. Participants were randomly divided into two groups, with fourteen of them first exposed to stress and then control condition and the other sixteen participants exposed to control before stress task. Participants did not significantly differ in age or gender across groups ($ps > 0.061$).

As shown in Fig. 1A, after an acclimation period of 10 min following arrival (T1), affect ratings were collected. Participants were then informed of the stress or control task (see *stress induction*) and were given 5 min to prepare for it. After preparation (T2), affect ratings were recorded. Participants went through the stress or control task, with affect ratings collected again upon task completion (T3). Next, there were 3 sessions of stop signal task (SST; see *stop signal task)*. Affect ratings were collected at the end of each SST session (T4, T5, and T6).

2.1.3. Stress induction

In the stress condition, participants completed the TSST, a well-validated task with stressors consisting of an impromptu speech and a mental arithmetic task (Kirschbaum et al., 1993). Participants were instructed to prepare an application for a job of their choice and to introduce themselves to the search committee (investigators) in a free speech of 5 min. They were to convince the committee that they were the most suitable candidate for this position. To increase task engagement, participants were asked to write down the speech during the preparation period and to deliver the speech without notes in front of a video camera and the committee (one woman and one man) who were trained to remain emotionally neutral. Without prior knowledge, they were then asked to subtract the number 13 serially from 1022 in English as fast and accurately as possible within 5 min in front of the same committee. On any error the committee asked the participant to start again at 1022. Reporting in a foreign language (i.e. English) should increase the difficulty of the mental arithmetic task in Chinese participants and possibly further enhance their stress level. In the control condition, to ensure a comparable cognitive load, participants went through the same tasks alone in the absence of the committee and video camera. In other words, there was no social evaluative stress in the control condition.

2.1.4. Stop signal task

We employed a stop signal task (Hu et al., 2016; Hu and Li, 2012).

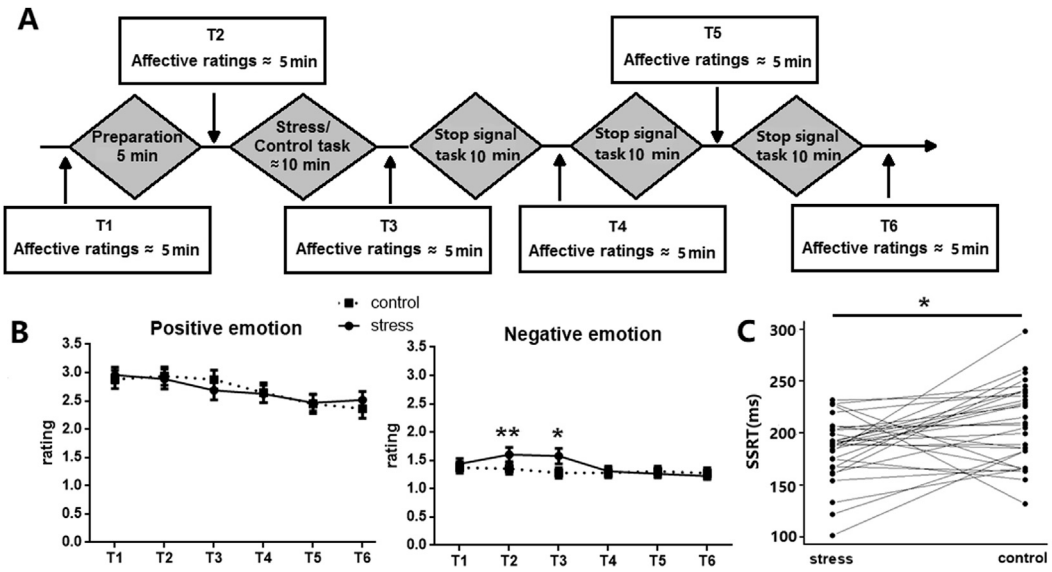

Fig. 1. Experimental procedure and results of the behavioral study (experiment 1). ***A***, The timeline of the experiment. ***B***, Positive/negative emotional responses under control and stress conditions (mean and standard error). ***C***, Stop signal reaction time (SSRT) under stress and control conditions for each participant. $^{*}p < 0.05$, $^{**}p < 0.01$, SSRT, stop signal reaction time.

Two types of trials, "go" and "stop", were randomly intermixed in presentation. There was an inter-trial interval of 2 s. A small dot appeared on the screen to signal the beginning of each trial. After a randomized interval varying from 1 to 5 s, the dot turned into a circle, the go signal, prompting participants to press a button quickly. The circle vanished at button press or after 1 s if the participants failed to respond. A premature button press prior to the appearance of the circle also terminated the trial. Approximately one quarter of the trials were stop trials, in which the go signal was followed by an "X" (the stop signal), instructing participants to withhold button press. Likewise, a trial terminated at button press or when 1 s had elapsed after the appearance of the stop signal. The stop signal delay (SSD), the time interval between the go and stop signals, started at 200 ms and varied from one stop trial to the next according to a staircase procedure, increasing and decreasing by 67 ms each after a successful and failed stop (Levitt, 1971). With the staircase procedure, we anticipated that the participants would succeed in withholding their response in approximately half of the stop trials. Participants were instructed to respond to the go signal quickly while keeping in mind that a stop signal might come up, and both accuracy and response speed were emphasized (Li, Huang, et al., 2008). Prior to the experiments, participants were trained on the same behavioral task. In the behavioral study, each participant completed three 10-min runs of the task with 100 trials in each run.

2.1.5. Psychological measure

In the behavioral experiment, positive and negative affect ratings (PANAS, including positive emotions: calm, relaxed, peaceful, confident, and energetic; negative emotions: nervous, anxious, scared, tired, and upset) were rated on a 5-point scale from 1 ("not at all") to 5 ("extremely") (van Marle et al., 2010; Watson et al., 1988) at multiple time points throughout the procedure. The positive and negative emotion ratings were analyzed using a repeated-measures ANOVA with treatment (control vs. stress) and time point (T1, T2, T3, T4, T5, and T6) as two within-subject factors, respectively. After adding age and gender as covariates, we found similar results. Hence, we only reported the results of ANOVA without these covariates in the results section. Further, we also conducted repeated-measures ANOVAs with task order (stress-first vs. control-first) as a between-subject factor, treatment and time point as two within-subject factors. We found the main findings, i.e., the interaction between treatment and time point, remained unchanged. For all reported analyses, Greenhouse-Geisser correction was applied when the assumption of sphericity was violated.

2.1.6. Behavioral data analysis

We computed the stop signal reaction time (SSRT) for each participant on the basis of the race model (Logan et al., 1984). The SSRT represents the time one requires to stop the button press after the stop signal appears. Shorter SSRT indicates better response inhibition. Firstly, we estimated the critical SSD, the delay that allows a participant to correctly inhibit response to a stop signal in half of the stop trials. SSDs across stop trials were grouped into runs (sequences of trials), with each run defined as a monotonically increasing or decreasing series. We derived a mid-run estimate by taking the middle SSD of every even run. The critical SSD was computed by taking the mean of all mid-run SSDs. The mid-run measure was reported close to the maximum likelihood estimate of 50% stop success in the SST with enough trails (more than 30) (Duann et al., 2009; Li, Yan, Sinha and Lee, 2008; Wetherill et al., 1966). Then, the SSRT was computed by subtracting the critical SSD from the median go trial reaction time (RT) (Hu and Li, 2012).

Four performance indexes of the SST, including go success rate, go trial reaction time, stop success rate and SSRT, were compared between stress and control condition using paired *t* tests.

2.1.7. Results

For positive and negative emotion ratings, we carried out treatment (control vs. stress) by time point (T1, T2, T3, T4, T5, and T6) repeated-measures ANOVAs (Fig. 1B and Table 1). For positive emotion ratings, the main effect of time point was significant ($F(5, 145) = 13.720$, $p < 0.001$, partial $\eta 2 = 0.321$). The main effect of treatment and the interaction between treatment and time point were not significant ($F(1, 29) = 0.002$, $p = 0.966$, partial $\eta 2 < 0.001$; $F(5, 145) = 1.957$, $p = 0.117$, partial $\eta 2 = 0.063$, respectively). For negative emotion ratings, the results showed a significant main effect of time point ($F(5, 145) = 5.879$, $p = 0.002$, partial $\eta 2 = 0.169$), and a significant interaction between treatment and time point ($F(5, 145) = 4.750$, $p = 0.007$, partial $\eta 2 = 0.141$). The main effect of treatment was not significant ($F(1, 29) = 1.673$, $p = 0.206$, partial $\eta 2 = 0.055$). Post-hoc *t*-tests revealed significantly higher negative emotion ratings in stress than in control condition at T2 ($t(29) = 3.167$, $p = 0.004$) and T3 ($t(29) = 2.366$, $p = 0.025$).

We evaluated performance in the SST. For go success rate, a paired *t*-test showed no difference between stress ($M \pm SD = 95.80 \pm 3.70\%$) and

Table 1
The results of affect ratings.

	T1	T2	T3	T4	T5	T6
	Mean(SD)	mean(SD)	mean(SD)	mean(SD)	mean(SD)	mean(SD)
Behavioral experiment						
PA						
Stress	2.96(0.77)	2.89(0.94)	2.69(0.89)	2.62(0.83)	2.47(0.80)	2.51(0.83)
Control	2.88(0.86)	2.94(0.87)	2.88(0.89)	2.64(0.95)	2.45(0.92)	2.36(0.91)
NA						
Stress	1.44(0.50)	1.60(0.67)	1.58(0.73)	1.31(0.49)	1.26(0.35)	1.22(0.32)
Control	1.37(0.54)	1.36(0.53)	1.28(0.49)	1.28(0.48)	1.30(0.51)	1.28(0.51)
fMRI experiment						
PA						
Stress	3.09(0.44)	2.71(0.59)	2.52(0.60)	2.66(0.63)	2.69(0.58)	2.93(0.62)
Control	3.07(0.47)	2.96(0.60)	3.05(0.60)	2.85(0.71)	2.67(0.66)	2.91(0.70)
NA						
Stress	1.57(0.41)	1.83(0.47)	1.97(0.56)	1.74(0.50)	1.67(0.46)	1.57(0.50)
Control	1.40(0.40)	1.46(0.46)	1.45(0.45)	1.57(0.61)	1.66(0.54)	1.60(0.58)

control ($M \pm SD = 96.10 \pm 2.90\%$) condition ($t(29) = -0.296$, $p = 0.770$). Across participants, the average go trial reaction time was 597.00 ± 90.00 ms and 601.00 ± 93.00 ms in stress and control condition, respectively, and there was no significant difference ($t(29) = -0.399$, $p = 0.693$). Analysis of stop success rate showed no difference between stress and control condition ($t(29) = -1.987$, $p = 0.056$). Notably, participants made errors in roughly half of the stop trials in both conditions (stress: $M \pm SD = 51.60 \pm 2.20\%$; control: $M \pm SD = 52.70 \pm 3.50\%$), suggesting that their overall performance was adequately tracked by the staircase procedure. Further, SSRT under stress ($M \pm SD = 185.00 \pm 31.00$ ms) was significantly shorter than under control condition ($M \pm SD = 208.00 \pm 38.00$ ms; $t(29) = -2.773$, $p = 0.010$), suggesting improved response inhibition under stress (Fig. 1C and Table 3). Compared with the control condition, twenty-three out of thirty participants required less time after stress exposure to stop the button press after the stop signal appeared (see Fig. 1C).

2.2. Experiment 2: an fMRI study

2.2.1. Participants

Thirty right-handed volunteers 20.6 ± 2.0 (mean $\pm$ SD; range 18–25) years of age, including 15 females, were recruited from the local community. None of the participants reported any history of major medical, psychiatric, or neurological diseases. None reported previous participation in stress-related research. No female participants reported any use of hormonal contraceptives. Participants were instructed to refrain from heavy exercise and caffeine for at least 12 h before the experiment. All participants provided written informed consent according to the study protocol approved by the South China Normal University Institutional Review Board.

2.2.2. Experimental design and procedure

As showed in Fig. 2A, after an acclimation period of 20 min following arrival (T1), baseline saliva samples and affect ratings were collected. Participants were then informed of the stress or control task *(see stress induction in experiment 1)* and were given 5 min of preparation time. After preparation (T2), affect ratings were recorded again. Participants went through the stress or control task, with saliva samples and affect ratings collected upon task completion (T3). Next, 8 min of resting-state fMRI data were collected. After completion of resting state fMRI scan, participants were engaged in 3 sessions of the SST (see *stop signal task in experiment 1*), and saliva samples and affect ratings were collected at the end of each SST session (T4, T5, and T6). Each session included 120 trials, with approximately 12 min to finish it. Then T1 images were scanned for about 5 min. All experiments were conducted between 1 and 6 p.m. to ensure a relatively low and stable level of endogenous cortisol. As with the behavioral study, participants received acute stress and control exposure in two separate sessions at least 30 days apart, and the order of exposure was counter-balanced across subjects. Participants were randomly assigned to two groups based on condition order, such that half completed the stress condition first and the other half completed the control condition first. Participants did not significantly differ in age or gender across groups ($ps > 0.5$).

2.2.3. Psychological and physiological measures

In the fMRI experiment, the positive and negative affect were recorded in the same way as did in the behavioral study (see *psychological measure in experiment 1*). Saliva samples were collected with the Salivettes (Sarstedt, Germany) and were stored at −15 °C until assayed. Cortisol concentrations in saliva (in ng/mL) were measured by ELISA (catalog No. SLV 4635; DRG, Germany).

The ratings for positive and negative emotion were fed to a repeated-measures ANOVA with treatment (control vs. stress) and time point (T1, T2, T3, T4, T5, and T6) as two factors, respectively. For saliva cortisol level, three participants' cortisol samples could not be assayed due to insufficient saliva, leaving data from 27 participants for a treatment (control vs. stress) by time point (T1, T3, T4, T5, and T6) repeated-measures ANOVA analysis. After adding age and gender as covariates, we found similar results, thus we only reported the analyses without these covariates in the results section. Further, we also conducted repeated-measures ANOVAs with task order (stress-first vs. control-first) as between-subject factor, treatment and time point as two within-subject factors on cortisol level, positive and negative emotion data. We found that the main findings, i.e., the interaction between treatment and time point, remained unchanged. For all reported analyses, Greenhouse-Geisser correction was applied when the assumption of sphericity was violated.

2.2.4. Behavioral data analysis

As in the behavioral study, we measured the SSRT as the index of response inhibition performance (see *behavioral data analysis 1*). Paired *t* tests were conducted to compare SSRT, go success rate, go trial reaction time, and stop success rate between stress and control condition.

2.2.5. Imaging protocol

Images were obtained with a 3-Tesla MRI scanner (Siemens) at the Brain Imaging Center at South China Normal University. The scanner was equipped with a 12-channel head coil. Anatomical images of the functional slice locations were obtained with spin echo imaging in the axial plane parallel to the AC-PC line with repetition time (TR) = 1900 ms,

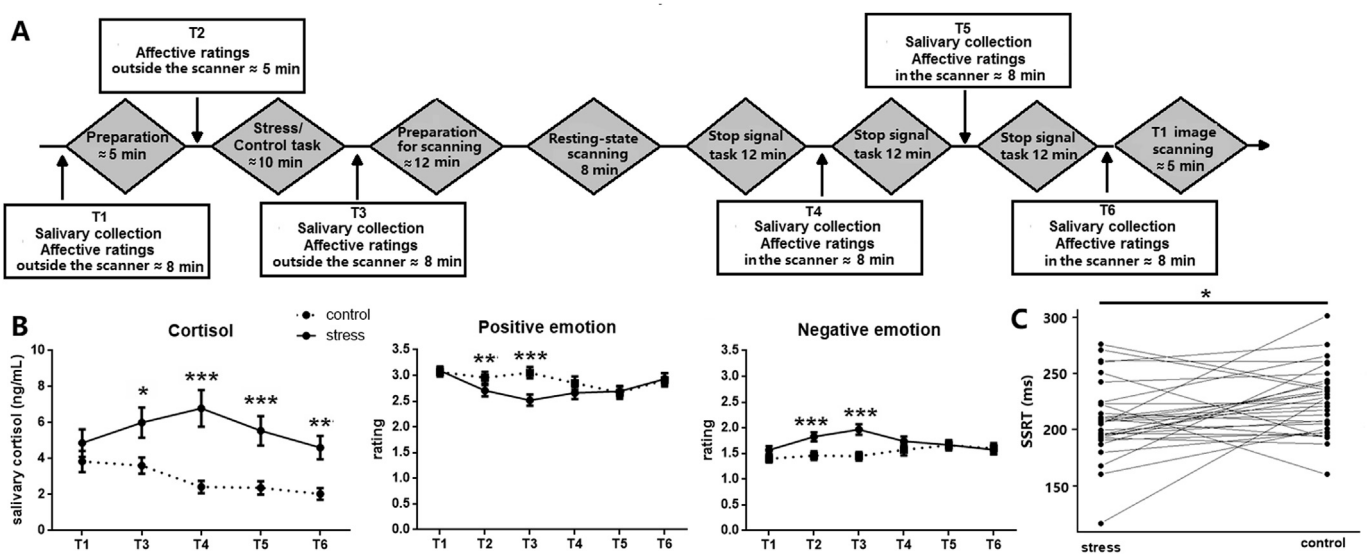

Fig. 2. Experimental procedure and behavioral results of the fMRI study (experiment 2). A, The timeline of the experiment. B, Cortisol and positive/negative emotional responses under control and stress conditions (mean and standard error). C, Stop signal reaction time (SSRT) under stress and control conditions for each participant. *$p < 0.05$, **$p < 0.01$, ***$p < 0.001$, SSRT, stop signal reaction time.

echo time (TE) = 2.52 ms, field of view = 256 × 256 mm^2, flip angle = 9°, matrix size = 256 × 256, and 1 mm^3 isotropic voxel. Functional, blood oxygenation level dependent (BOLD) signals were acquired with a single-shot gradient echo echo-planar imaging (EPI) sequence. Thirty-two axial slices parallel to the AC-PC line covering the whole brain were acquired with TR = 2000 ms, TE = 25 ms, flip angle = 85°, field of view = 220 × 220 mm, matrix = 64 × 64, in-plane voxel size = 3 × 3 mm, and slice thickness = 4 mm with no gap. Slice scanning order was ascending interleaved. Three hundred and sixty images were acquired in each run for three runs.

2.2.6. *Imaging data processing*

The fMRI data was preprocessed and analyzed using Statistical Parametric Mapping version 8 (SPM8, Wellcome Department of Imaging Neuroscience, University College London, U.K.). To allow for equilibration effects, the first five volumes were discarded. The remaining images were firstly corrected for slice timing and realigned (motion-corrected). A mean functional image volume was constructed for each participant for each run from the realigned image volumes. These mean images were co-registered with the high-resolution structural image and segmented for normalized to an MNI (Montreal Neurological Institute) EPI template with affine registration followed by nonlinear transformation (Ashburner and Friston, 1999; Friston et al., 1995). Finally, images were smoothed with a Gaussian kernel of 8 mm at full width at half maximum. The data was high-pass filtered (1/128 Hz cutoff) to remove low-frequency signal drifts.

2.2.7. *General linear model (GLM)*

In GLM of the BOLD signals, four events – go success (GS), go error (GE), stop success (SS), and stop error (SE) – were modeled and the go signal onsets were convolved with a canonical hemodynamic response function (HRF) and the temporal derivative of the canonical HRF (Friston et al., 1994). GS trials were parametrically modulated by the reaction time and its temporal derivative. SS and SE trials were parametrically modulated by the SSD and its temporal derivative (Büchel et al., 1998; Hu and Li, 2012; Li et al., 2006). Previous studies found that including these parametric modulators could improve model fit (Cohen, 1997; Hu, Ide, Zhang, Sinha, & Chiang-shan, 2015; Hu and Li, 2012). Six head-motion parameters defined by the realignment were added to the model as regressors of no interest and serial auto-correlation was corrected by a first-degree autoregressive or AR(1) model (Della-Maggiore et al., 2002; Friston et al., 2000).

In the first-level analysis, we contrasted SS versus SE (SS > SE) for each participant to identify the neural correlates of response inhibition. The SS and SE trials were identical in stimulus condition, with each involving inhibition success and failure, respectively. The contrast SS > SE thus engaged the processes related to response inhibition (Duann et al., 2009; Farr, Hu, Zhang, & Chiang-shan, 2012; Li, Yan, et al., 2008). A random effects analysis (one-sample *t*-test) was performed to identify regional activations for SS versus SE contrast at group level each during stress and control condition. A conjunction analysis of SS - SE contrasts under both stress and control conditions was conducted to identify activations shared across these two conditions. A paired *t*-test of the *con* or contrast (difference in β) images of SS minus SE was employed to compare regional activations between stress and control condition.

In addition to exploring stress-induced changes in independent regions of the network related with response inhibition, we also examined whether different connectivity flows were involved in stress and control condition during inhibition process by conducting a psychophysiological interaction (PPI) analysis. The PPI analysis identified how functional connectivity between pairs of brain regions modulated by psychological context (i.e. SS and SE in the present study) (Friston et al., 1997). The source regions used in the PPI analysis were defined as 6 mm spheres centered at the peak voxel of the group-level conjunction results of SS vs. SE under stress and control condition. Participant-specific PPI models were performed for each source region with 3 regressors of (1) the main effect of seed region activity (physiological), (2) the main effect of response inhibition motivation (SS-SE, psychological), and (3) the interaction effect of seed region activity by the response inhibition motivation (PPI), each corresponding to PPI.Y, PPI.P, and PPI.ppi in the design matrix. Six head-motion parameters were also added to the model as regressors of no interest. Contrast images were generated for positive and negative PPIs, which indicated the identified regions had greater or lesser coupling with the source regions according to the context of SS versus SE condition.

The PPI first-level contrast (positive and negative PPIs) for each source region in stress and control condition were fed into 2 s-level GLM analyses: (1) exploring the brain regions whose connectivity with source regions for SS versus SE context varied under stress and control condition (paired *t*-test); (2) identifying regions of which the stress-related changes in connectivity with the source regions in SS – SE context varied as a function of individual differences in SSRT between stress and control

condition ("higher-order" PPI). For higher-order PPI analysis, we performed a whole-brain regression with "SSRT under stress – SSRT under control" as the independent variable and stress-induced changes in PPI (positive PPI contrast under stress-positive PPI contrast under control) in SS – SE context as the dependent variable (Passamonti et al., 2008, 2009).

For all reported analyses, we included age, gender and the order of conditions (stress or control first) as covariates. The results were evaluated at a threshold of voxel-level family-wise error (FWE) corrected $p < 0.05$ using small volume correction (SVC) on images with an uncorrected voxel threshold of $p < 0.001$. Based on previous studies, there were 10 ROIs for SVC, including bilateral inferior frontal gyrus (IFG), superior frontal gyrus (SFG), middle frontal gyrus (MFG), putamen and caudate (Bari and Robbins, 2013; Courtney et al., 2013; Ghahremani et al., 2012), all defined using the corresponding AAL mask (Tzourio-Mazoyer et al., 2007). Each ROI was tested separately in SVC, and the results were examined with Bonferroni correction for multiple comparisons, i.e., $p < 0.005$ (0.05/10).

2.2.8. Dynamic causal modelling (DCM) analysis

To test the direction of information flow in the brain network found by PPI analyses, we conducted a DCM analysis (Friston, Harrison and Penny, 2003). The DCM is a hypothesis-driven approach to assess effective connectivity among brain regions and their context-dependent modulation (Friston et al., 2003; Seghier et al., 2010).

The nodes as identified from brain network found using PPI analyses included the right SFG/MFG, and the left putamen and caudate (see Results). Firstly, we made masks for these nodes by overlapping peak activation voxels (left putamen and caudate from PPI; and right SFG/MFG from conjunction; radius = 6 mm) and the corresponding masks from the AAL template to ensure the anatomical locations of the nodes. Secondly, considering inter-subject variability, VOIs in spheres of 5 mm radius were defined centered on participant-specific maxima in these masks. For the stop success (i.e., SS) condition, we specified a three-area DCM using the VOIs as defined above (Fig. 4A). To identify the best family of model fits, we conducted a random effects family inference analysis. The signals of SS entered the network (driving inputs) though the striatum node (i.e., putamen and caudate), or the PFC (right SFG/MFG) node, or both. Based on the driving inputs, we had three families of models, including both striatum and PFC inputs (model 1-model 6), PFC-only inputs (model 7–12), and striatum-only inputs (the model 13–18) (Nicholson et al., 2017) (see Fig. 4). Further, we assumed that the SS condition modulated 1) only the connectivity from striatum to PFC without the internal connectivity between caudate and putamen; 2) only the connectivity from PFC to striatum without the internal connectivity between caudate and putamen; 3) both connectivity from PFC to striatum and from striatum to PFC without the internal connectivity between caudate and putamen; 4) only the connectivity from striatum to PFC with the internal connectivity between caudate and putamen; 5) only the connectivity from PFC to striatum with the internal connectivity between caudate and putamen; 6) both connectivity from PFC to striatum and from striatum to PFC with the internal connectivity between caudate and putamen.

The Bayesian model selection (BMS) procedure was used to determine the best model at the group level; that is, we compared the model evidence for all 18 predefined models. We applied a random-effects BMS approach, which was found to be robust in coping with potential outliers (Stephan et al., 2009). The model evidence represents the probability of generating the observed data by a specific model (Penny et al., 2004). A common method to compare evidence among different models is given by the exceedance probability (EP); i.e., given the group data, the probability that a specific model is more likely than any other tested models (Schmidt et al., 2016). The EP is intuitive as all EPs sum to one over all tested model. The model with the highest EP is considered as the best model (Nicholson et al., 2017; Penny et al., 2010; Seghier and Price, 2009). We also used the random-effects BMS to determine the best family. The EP of a family is sum of the EPs of all models included in this family. Likewise, the family with the highest EP was the most likely one according to the data from all subjects (Penny et al., 2010).

2.2.9. Brain-behavior correlation analysis

Correlations between the cortisol level or affect ratings and brain activation or effective connectivity were examined. Significant correlations were reported at $p < 0.05$ Bonferroni-corrected.

3. Results

3.1. Physiological and behavioral responses to acute stress

We carried out treatment (control vs. stress) by time point (T1, T3, T4, T5, and T6) repeated-measures ANOVA on cortisol level (Fig. 2B and Table 2). Results showed that the main effects of treatment (F (1, 26) = 16.258, $p < 0.001$, partial $\eta 2 = 0.385$) and time point ($F(4, 104) = 4.159$, $p = 0.010$, partial $\eta 2 = 0.138$) were significant. The interaction between treatment and time point was also significant ($F(4, 104) = 4.453$, $p = 0.006$, partial $\eta 2 = 0.146$). Post-hoc t-tests showed that stress as compared to control condition induced higher cortisol at T3 ($t(26) = 2.677$, $p = 0.013$), T4 ($t(26) = 4.503$, $p < 0.001$), T5 ($t(26) = 4.112$, $p < 0.001$) and T6 ($t(26) = 3.947$, $p = 0.001$).

For positive and negative emotion ratings, we also carried out treatment (control vs. stress) by time point (T1, T2, T3, T4, T5, and T6) repeated-measures ANOVAs (Fig. 2B and Table 1). For positive emotion ratings, the main effects of treatment ($F(1, 29) = 4.355$, $p = 0.046$, partial $\eta 2 = 0.131$) and time point ($F(5, 145) = 6.556$, $p < 0.001$, partial $\eta 2 = 0.184$) were significant; and the interaction between treatment and time point was also significant ($F(5, 145) = 7.505$, $p < 0.001$, partial $\eta 2 = 0.206$). Post-hoc t-tests showed that positive affect was lower in the stress than control condition at T2 ($t(29) = -2.801$, $p = 0.009$), and T3 ($t(29) = -4.817$, $p < 0.001$). For negative emotion ratings, the results revealed significant main effects of treatment (F (1, 29) = 8.553, $p = 0.007$, partial $\eta 2 = 0.228$) and time (F (5, 145) = 3.354, $p = 0.015$, partial $\eta 2 = 0.104$). The interaction between treatment and time was also significant (F (5, 145) = 7.495, $p < 0.001$, partial $\eta 2 = 0.205$). Post-hoc t-tests revealed significantly higher negative emotion ratings in stress than in control condition at T2 ($t(29) = 4.413$, $p < 0.001$) and T3 ($t(29) = 4.763$, $p < 0.001$). Taken together, these findings confirmed that acute stress enhanced cortisol level and modulated emotional experience.

In SST performance, a paired t-test analysis showed no difference between stress ($M \pm SD = 94.47 \pm 4.80\%$) and control conditions ($M \pm SD = 93.89 \pm 4.21\%$) in go success rate ($t(29) = 0.532$, $p = 0.599$). Across participants, the average go trial reaction time did not differ between stress (619.04 ± 108.36 ms) and control (620.23 ± 86.73 ms) conditions ($t(29) = -0.071$, $p = 0.944$). Analysis of success stop rate showed that participants made errors in roughly half of the stop trials in both stress ($M \pm SD = 50.95 \pm 3.59\%$) and control conditions

Table 2
The results of cortisol level in fMRI experiment.

	T1	T3	T4	T5	T6
	Mean(SD)	mean(SD)	mean(SD)	mean(SD)	mean(SD)
Stress	4.87(3.96)	6.01(4.38)	6.80(5.30)	5.55(4.27)	4.61(3.36)
Control	3.84(3.04)	3.61(2.32)	2.43(1.80)	2.38(1.94)	2.04(1.68)

Table 3
The results of SSRT.

	Stress	Control
	Mean(SD)	Mean(SD)
Behavioral experiment	185.15(30.78)	208.41(38.42)
fMRI experiment	209.00(33.20)	224.77(29.56)

($M \pm SD = 51.53 \pm 2.08\%$; $t(29) = -0.921$, $p = 0.365$), suggesting that their overall performance was adequately tracked by the staircase procedure. Further, as with the behavioral study, SSRT under stress ($M \pm SD = 209.00 \pm 33.20$ ms) was significantly shorter than under control ($M \pm SD = 224.77 \pm 29.56$ ms; $t(29) = -2.141$, $p = 0.041$), suggesting more efficient response inhibition after stress exposure (Fig. 2C and Table 3). After the stop signal appeared, twenty-one of all participants (i.e., 30) required less time in the aftermath of stress to stop the button press compared with the control condition (see Fig. 2C).

3.2. Imaging GLM results

As hypothesized, in the stress condition, one-sample *t*-test showed that SS as compared to SE involved higher activities in the left SFG ([-24 35 46], voxel = 227, $p < 0.001$, SVC), right SFG ([27 44 40], voxel = 153, $p < 0.001$, SVC), left MFG ([-30 41 31], voxel = 247, $p < 0.001$, SVC), right MFG ([27 44 43], voxel = 257, $p < 0.001$, SVC) and other regions (Fig. 3A, left panel). In the control condition, one-sample *t*-test of SS minus SE engaged the left SFG ([-24 35 46], voxel = 134, $p < 0.001$, SVC), right SFG ([24 38 52], voxel = 90, $p = 0.001$, SVC), left MFG ([-24 32 52], voxel = 112, $p < 0.001$, SVC), right MFG ([33 38 40], voxel = 197, $p < 0.001$, SVC) and other regions (Fig. 3A, right panel). Since the voxels that showed significant differences in ipsilateral SFG and MFG were neighboring voxels, we combined the left SFG and MFG to left SFG/MFG ROI, right SFG and MFG to right SFG/MFG ROI, and carried out small volume correction again. The results showed that the activities of left and right SFG/MFG were significantly higher for SS vs. SE in stress ([-30 41 31], voxel = 466, $p < 0.001$, SVC; [27 44 43], voxel = 319, $p < 0.001$, SVC) and in control ([-24 32 52], voxel = 240, $p < 0.001$, SVC; [33 38 40], voxel = 197, $p < 0.001$, SVC) condition (Table 4). Conjunction analysis for contrasts of SS vs. SE under stress and control conditions revealed activations in left and right SFG/MFG ([-27 35 46], voxel = 284, $p < 0.001$, SVC; [30 41 40], voxel = 210, $p < 0.001$, SVC) (Fig. 3B and Table 4). Further, paired *t*-test showed no significant differences for the stress minus control and control minus stress contrast in the regions of interest, suggesting a similar involvement of the SFG/MFG (Table 4). No significant correlations between brain activity under stress and stress-induced salivary cortisol level ($stress_{(T4\text{-}T1)}$, $stress_{(T5\text{-}T1)}$ and $stress_{(T6\text{-}T1)}$) and emotion ratings ($NA_{(T4\text{-}T1)}$, $NA_{(T5\text{-}T1)}$, $NA_{(T6\text{-}T1)}$, $PA_{(T4\text{-}T1)}$, $PA_{(T5\text{-}T1)}$ and $PA_{(T6\text{-}T1)}$) were found (all $ps > 0.05$).

Using the left and right SFG/MFG as seeds, we conducted PPI analyses in stress and control group, respectively. The pair *t* tests showed that no region of interest showed significantly different connectivity with the PPI seeds in SS minus SE context between stress and control conditions (Table 4). The higher-order PPI results showed that stress-induced changes in response inhibition (SSRT under stress – SSRT under control) was negatively correlated with stress-induced changes (stress minus control) in connectivity between the left SFG/MFG seed and left caudate ([-12 14–2], voxel = 3, $p = 0.035$, SVC) (Fig. 3C, left; Table 4). For the right SFG/MFG seed, the stress-related changes in the connectivity between right SFG/MFG and left putamen and bilateral caudate (left putamen: [-18 17–2], voxel = 20, $p = 0.005$, SVC; right caudate: [12 20–2], voxel = 4, $p = 0.044$, SVC; left caudate: [-15 20 1], voxel = 37, $p = 0.002$, SVC) were negatively correlated with stress-induced changes in response inhibition (Fig. 3C, middle and right panels; Table 4). These high-order PPI findings show that shorter SSRT in stress as compared with control condition was associated with stronger connectivity between SFG/MFG seeds and the striatum. We focused on the connectivity findings surviving Bonferroni correction for multiple SVC analyses ($p < 0.05/10$) in the DCM analysis; i.e., the connectivity between right SFG/MFG and left caudate and putamen.

3.3. DCM results

After identifying the SFG/MFG and SFG/MFG – striatal connectivity as critical to the inhibition process, we applied DCM to test causal connectivities within the network. As shown in Fig. 4B, the second family fitted the data best under both stress and control conditions, in which SS signals entered the models (model 7–12) through right SFG/MFG. Specifically, the second family yielded an exceedance probability (xP) = 1 in stress, and $xP = 0.998$ in control condition (Fig. 4B). Further, in stress, model 12 outperformed all other models with an exceedance probability of 58%, where experimental context (i.e., SS) entered the network though the right SFG/MFG node and modulated all modeled connectivities, including connectivity from left caudate to right SFG/MFG, from left putamen to right SFG/MFG, from left caudate to left putamen, from

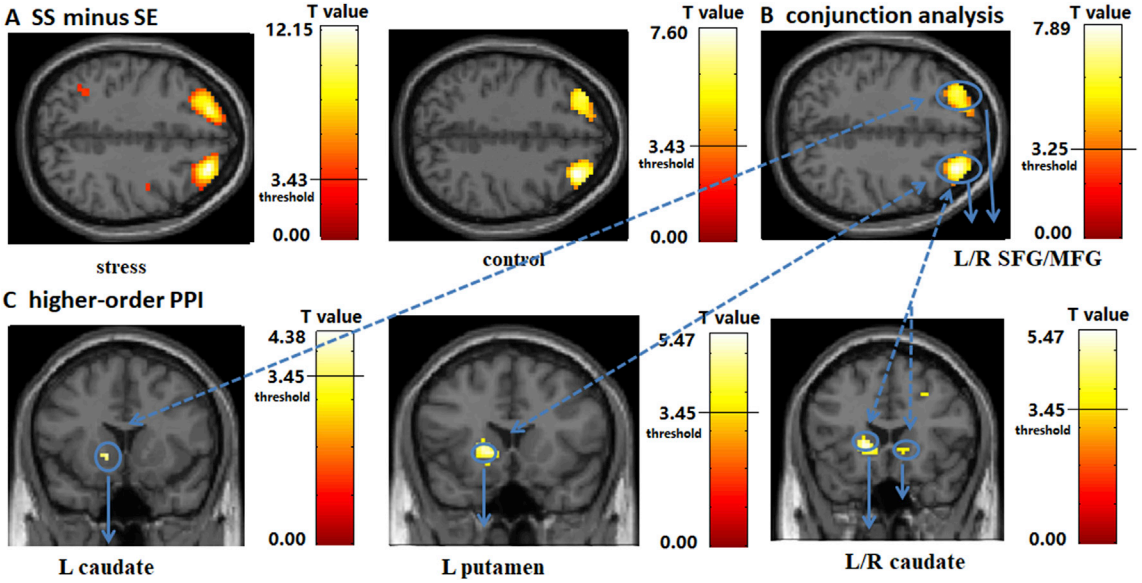

Fig. 3. *A*, Regional responses to SS vs. SE under both stress and control conditions; ***B***, Conjunction analysis for contrasts of SS versus SE under stress and control condition; ***C***, The results of higher-order PPI. Participants with shorter SSRT (stress condition minus control condition) showed stronger connectivity between left SFG/MFG seed and left caudate ([-12 14–2], voxel = 3, $p = 0.035$, SVC), and between right SFG/MFG and left putamen and bilateral caudate (left putamen: [-18 17–2], voxel = 20, $p = 0.005$, SVC; right caudate: [12 20–2], voxel = 4, $p = 0.044$, SVC; left caudate: [-15 20 1], voxel = 37, $p = 0.002$, SVC). L, left; R, right; SS, stop success; SE, stop error; SFG/MFG, superior/middle frontal cortex; PPI, psychophysiological interaction.

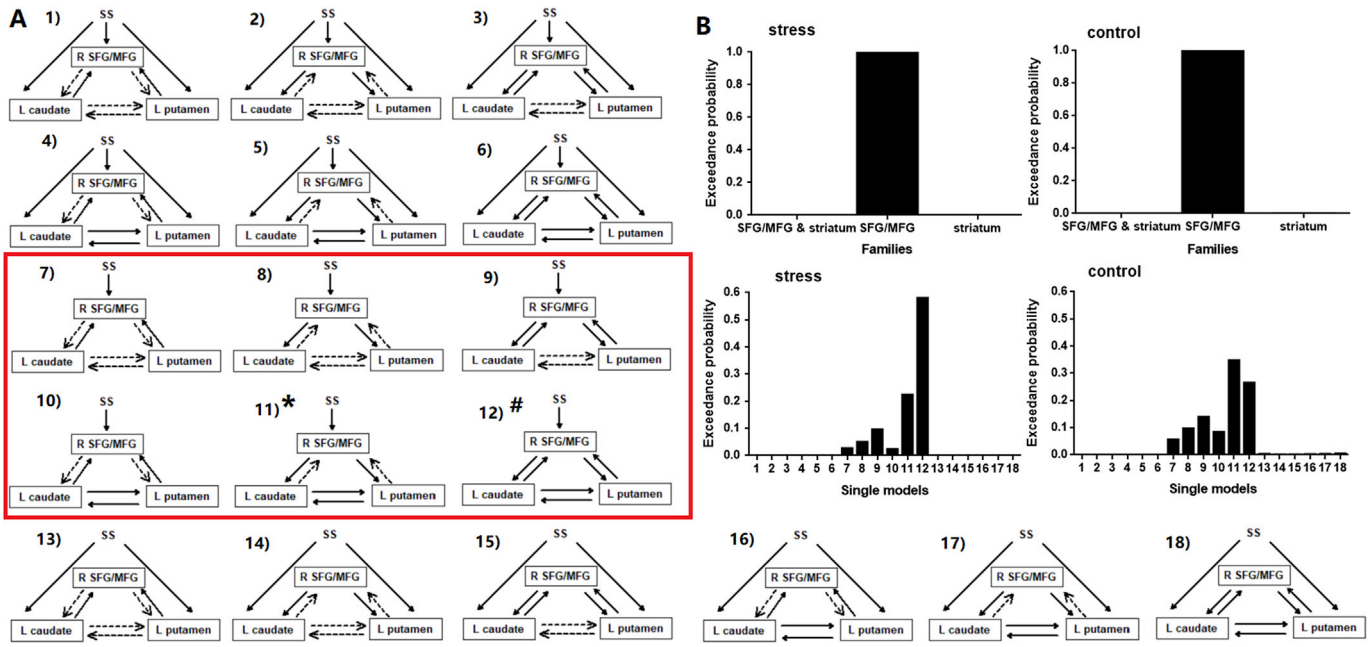

Fig. 4. *A*, The 18 models tested in the dynamic causal model (DCM) analysis. Using Bayesian model selection procedure, model 11 was the best model under control condition, while model 12 fit the data best under stress condition. The 18 models were derived from different combinations of signal input (either in SFG/MFG, in striatum, or in both) and causal information flow. The solid line with arrows indicated the information flow, while the dotted line represented the effective connectivity that was not included in the models. Models were grouped in families based on their driving inputs (1) models with both striatum and SFG/MFG inputs (model 1 to 6), (2) models with only SFG/MFG inputs (model 7 to 12), (3) models with only striatum inputs (model 13 to 18). The second family highlighted in a red box fit the data best under both stress and control conditions. ***B***, The exceedance probability of each family/model under stress and control conditions. The second family yielded an exceedance probability (xP) = 1 under stress and an xP = 0.998 in control condition. Model 12 outperformed all other models with an exceedance probability of 58% under stress condition. For the control condition, the model 11 fit the data best with an exceedance probability of 35%. R, right; SS, stop success; SFG/MFG, superior/middle frontal cortex; *best model for control condition; #best model for stress condition.

Table 4
fMRI results.

		Contrast	Brain Regions	Peak Z	Peak Coordinate MNI (X, Y, Z)	Volume (voxel)
One sample *t*-test	Stress	SS vs. SE	L SFG/MFG*[b]	6.650	−30, 41, 31	466
			R SFG/MFG*[b]	6.900	27, 44, 43	319
	Control	SS vs. SE	L SFG/MFG*[b]	6.890	−24, 32, 52	240
			RSFG/MFG*[b]	5.470	33, 38, 40	197
Two sample *t*-test	Stress-control	Stress (SS vs. SE) –Control (SS vs. SE)	No significant activation			
	Control-stress	Control (SS vs. SE) –Stress (SS vs. SE)	No significant activation			
Conjunction analysis	Stress ∩ Control	Stress (SS vs. SE) ∩ Control (SS vs. SE)	LSFG/MFG*[b]	6.110	−27, 35, 46	284
			RSFG/MFG*[b]	6.420	30, 41, 40	210
PPI analysis using L SFG/MFG as seed	Stress-Control	Stress (PPI.ppi) –Control (PPI.ppi)	No significant activation			
	Control-Stress	Control (PPI.ppi) –Stress (PPI.ppi)	No significant activation			
PPI analysis using R SFG/MFG as seed	Stress-Control	Stress (PPI.ppi) –Control (PPI.ppi)	No significant activation			
	Control-Stress	Control (PPI.ppi) –Stress (PPI.ppi)	No significant activation			
Higher-order PPI using L SFG/MFG as seed	Whole-brain regression	Positive	No significant activation	3.370	−12, 14, −2	3
		Negative	L caudate*			
Higher-order PPI using R SFG/MFG as seed	Whole-brain regression	Positive	No significant activation	4.010	−18, 17, −2	20
		Negative		3.290	12, 20, −2	4
			L putamen*[b]	4.190	−15, 20, 1	37
			R caudate*			
			L caudate*[b]			

*[b] survived for small volume correction $p < 0.001$ and Bonferroni correction $p < 0.005$; *small volume correction $p < 0.001$; SS, stop success; SE, stop error; L, left; R, right; SFG, superior frontal gyrus; MFG, middle frontal gyrus; PPI, psychophysiological interaction.

left putamen to left caudate, and from right SFG/MFG to left caudate and to left putamen. For the control condition, model 11 fitted the data best with an exceedance probability of 35%, which was characterized by information input to the right SFG/MFG with SS modulating most of modeled connectivities, except the connectivity from left caudate and putamen to right SFG/MFG (Fig. 4). The best models under stress and control conditions were not identical, which might suggest that the activation and connectivity patterns of the fronto-striatal circuit during successful stopping was altered after stress exposure (Seghier and Price, 2009). We found no significant correlations between the stress-related DCM connectivity parameters and stress-induced salivary cortisol level ($stress_{(T4\text{-}T1)}$, $stress_{(T5\text{-}T1)}$ and $stress_{(T6\text{-}T1)}$) and emotion ratings ($NA_{(T4\text{-}T1)}$, $NA_{(T5\text{-}T1)}$, $NA_{(T6\text{-}T1)}$, $PA_{(T4\text{-}T1)}$, $PA_{(T5\text{-}T1)}$ and $PA_{(T6\text{-}T1)}$) (all $ps > 0.05$).

4. Discussion

The present study examined the effect of acute psychosocial stress on response inhibition and its underlying neural mechanisms. The behavioral results of both studies showed that the SSRT was shorter in stress than in control condition, suggesting that acute stress improves response inhibition. The fMRI results indicated that prefrontal cortical (i.e., bilateral SFG/MFG) activations increased during successful versus unsuccessful stopping under both stress and control conditions. Furthermore, the high-order PPI results showed that stress-induced changes in response inhibition (SSRT under stress – SSRT under control) was negatively correlated with stress-induced changes (stress minus control) in connectivity between the PFC and striatum (i.e., left SFG/MFG and left caudate; right SFG/MFG and bilateral caudate, right SFG/MFG and left putamen), indicating that shorter SSRT in stress compared with control condition was associated with stronger connectivity between the SFG/MFG and dorsal striatum across individuals. Finally, DCM showed that the best models under stress and control condition were different, such that the effective connectivity between the SFG/MFG and striatum was more intense after stress exposure.

Consistent with the hypothesis, both the behavioral and fMRI experiments found stress-induced improvement in response inhibition, as reflected in shorter SSRT under stress in comparison with control condition. These findings are consistent with previous behavioral and electrophysiological findings of stress-related enhancement of response inhibition (Dierolf et al., 2017; Dierolf et al., 2018; Qi et al., 2017; Schlosser et al., 2013; Schwabe et al., 2013; Shields et al., 2016a,b). For example, healthy participants receiving hydrocortisone as compared to placebo demonstrated better performance in an emotional go/no-go task (Schlosser et al., 2013). In electroencephalography, inhibition-related ERP components (i.e., N2 and P3) were enlarged under stress, suggesting improvement of inhibition function after acute stress exposure (Dierolf et al., 2017, 2018; Qi et al., 2017). For instance, in a recent ERP study combining the TSST and a go/no-go task, acute stress improved response inhibition, as reflected in higher accuracy in compatible trials and enhanced N2/N2d and P3/P3d components in no-go vs. go trials (Dierolf et al., 2018). The enhanced inhibition of inappropriate behaviors after acute stress exposure may help individuals reallocate the cognitive resources and manage the stressors (Shields et al., 2016a,b). However, some studies reported no or deleterious effects of stress on response inhibition (Jiang and Rau, 2017; McGrath et al., 2016; Roos et al., 2017; Scholz et al., 2009; Starcke et al., 2016). For example, McGrath et al. found that the acute stress had no effects on the SST performance in heavy drinkers (McGrath et al., 2016). Using TSST, a previous study found the significant task practice effect observed in the control group for post-SST vs. pre-SST disappeared after stress exposure, suggesting that acute stress impairs the inhibition control (Roos et al., 2017). However, their TSST only involved the public speaking task. The additional mental arithmetic task in our study may induce stronger stress than that in Roos et al. study. Further, the authors explored the immediate effects of stress on inhibition by conducting SST immediately after TSST. The 30 min between the TSST and SST in the present study may allow the cortisol level to build up and reach the peak when the cognitive task was implemented. More works are clearly needed to fully understand the effects of acute stress on cognitive control under various influence factors.

Both stress and control conditions engaged the SFG/MFG during response inhibition, in accord with earlier reports of the roles of these prefrontal regions in the SST and go/no-go tasks (Duann et al., 2009; Zheng et al., 2008). We further found no condition difference in these regional activities, suggesting that the SFG/MFG were engaged in the task to a comparable degree at the group level. However, the high-order PPI results indicated that stress-induced improvement in SSRT was associated with the stress-induced changes in the strength of connectivity between the SFG/MFG and dorsal striatum (including caudate and putamen). These findings suggest that the acute stress-elicited enhancement in response inhibition might be associated with alteration of fronto-striatal connectivity, though not averaged changes in activation in individual brain regions. These findings are broadly consistent with previous work supporting a role of the fronto-striatal pathway in response inhibition (Courtney et al., 2013; Jahfari et al., 2011; Zandbelt and Vink, 2010). For example, a previous study of PPI found that the striatum was more strongly correlated with the right IFG in activation during successful as compared with unsuccessful inhibitions (Zandbelt and Vink, 2010). Individuals with alcohol misuse are considered to have poor response inhibition (Hu et al., 2016; Lawrence et al., 2009; Li, Luo, Yan, Bergquist and Sinha, 2009). A study found that the alcohol dependence severity was negatively correlated with the functional connectivity between putamen and prefrontal cortex during the SST, suggesting that fronto-striatal pathways may be compromised by alcohol abuse during response inhibition (Courtney et al., 2013). Along with these earlier studies, the current findings support a critical role of the PFC-striatal circuit in response inhibition and extend the literature by showing that the enhancement effects of acute stress on response inhibition are associated with frontostriatal connectivity.

We further conducted a DCM analysis to test stress-induced changes of directional information flow between the PFC and striatum, i.e., the right SFG/MFG, left caudate and left putamen, as identified by higher order PPI analysis. The DCM results showed that the family in which SS signals entered the models through right SFG/MFG fitted the data best under both stress and control conditions, suggesting the top-down regulation during successful stopping. Further, the DCM results highlighted different "best" models for stress and control condition, which would mean the pattern of fMRI activations under these two conditions were fitted by two different model structures (Seghier et al., 2010). Specifically, other than modulating the connectivity from left caudate to left putamen, from left putamen to left caudate, from right SFG/MFG to both left caudate and left putamen, stop success (SS) also modulated the connectivity from left caudate and left putamen to right SFG/MFG in stress but not in the control condition. These results are in line with the PPI results that the communication between SFG/MFG and striatum was enhanced after stress exposure, and provide additional support that stress improved the interaction between frontal cortex and striatum by facilitating the information flow from striatum to the PFC during successful inhibition. Also in accord, Jahfari et al. found that the model with effective connectivity between right IFG and right caudate fit the brain activation patterns better than the model without this pathway, and the strength of this effective connectivity was negatively associated with SSRT (Jahfari et al., 2011). To our knowledge, this is the first study to demonstrate that stress enhanced effective connectivity of fronto-striatal pathway during successful stopping. As DCM is a model-driven approach (Friston et al., 2003), it is worth noting that there might be other neural interconnections related to response inhibition under stress. It would be beyond the scope of this research to examine all possible connectivities, thus we focused on the effective connectivity between the brain regions identified in group analyses.

The enhanced response inhibition after acute stress exposure is consistent with the effect of acute stress on other areas, particularly on

memory and decision-making. For example, recent neuroimaging studies found that stress has favored the striatum-based procedural memory system over the hippocampus-based cognitive memory system, with a decrease in hippocampus activity and intact striatum cortex activity under stress (Schwabe et al., 2012; Schwabe and Wolf, 2012). The habitual behavior is not necessary to be bad, for it could improve response efficiency and thus be conductive to coping with current stress, especially in healthy individuals (Schwabe and Wolf, 2011). In social situations, people under stress also tend to make habitual decisions instead of engaging in goal-directed behaviors, being less likely to examine and rethink intuitive responses (Yu, 2016). It was found that individuals after acute stress showed more cooperation and generosity, which might be adaptive for survival under stress (Rand et al., 2012; Takahashi et al., 2007; Von Dawans, Fischbacher, Kirschbaum, Fehr and Heinrichs, 2012). All these lines of evidences suggested that acute stress could improve the ability of individuals to adapt to threaten surroundings. However, chronic stress could impair various cognitive functions, like inhibition and memory, and lead to psychopathological diseases such as post-traumatic stress disorder (PTSD) or major depressive disorder (MDD) in extreme circumstances (Mani et al., 2013; Mizoguchi et al., 2000).

Dysfunctional inhibition control has been commonly found in multiple pathological states, including obsessive compulsive disorder (OCD), attention deficit hyperactivity disorder (ADHD) and substance use disorder. Stress is considered as an important factor in the development and maintenance of these disorders (Courtney et al., 2013; Liston et al., 2006; Quirarte et al., 2009; Schwabe et al., 2013). A study found that after the TSST, ADHD patients reported feeling more intense stress than the control group, indicating they were more sensitive to stressors (Liston et al., 2006). As far as we know, our study is the first one to explore the neural mechanisms underlying the effect of acute stress on response inhibition and may pave the way for future research on cognitive control in patients with stress-related psychiatry disorders.

It is worth noting that there are some limitations in the present study. Firstly, there were only 30 healthy participants in both behavioral and fMRI experiments. Future studies are recommended to employ larger sample sizes to explore the effect of stress on response inhibition. Secondly, more comprehensive indexes for assessing stress level are needed. We found that the significant differences of emotional responses between stress and control condition disappeared during the SST (see Figs. 1B and 2B), possibly due to the fast decline of mood (74–80% decline after 16 s) (Garrett and Maddock, 2001). However, the cortisol level was significantly higher under stress condition throughout the scanning process, possibly due to the slow change in cortisol levels. Other stress indexes, such as heart rate and blood pressure, should be used in future studies to better understand the dynamic stress-induced physiological changes. Thirdly, we did not control the menstrual status of female participants. Although there are many studies showing the influences of menstrual cycle-related hormonal on cortisol level (Andreano et al., 2008; Duchesne and Pruessner, 2013), Kuhlmann and Wolf found that cortisol level was not significantly different between the mensis phase group and luteal phase group after the female participants receiving stress treatment (Kuhlmann and Wolf, 2005). Future studies are needed to further explore the effect of the menstrual cycle on the cortisol level. Finally, we found no significant correlations between stress-induced salivary cortisol levels or emotion ratings and brain activation or DCM parameters. This might be due to the relatively small sample size in our study. It is also possible that stress impacts cognition through more biological mechanisms (Shields et al., 2016a,b), including the hypothalamo-pituitary-adrenal (HPA) axis as well as the immune system (Steptoe et al., 2007) and parasympathetic nervous system (Roos et al., 2017).

In conclusion, the study demonstrated that acute stress improved response inhibition in the SST. Acute stress enhanced functional and effective connectivity between the SFG/MFG and striatum to support improvement in response inhibition. These findings may have broad implications for the research of frontostriatal circuit dysfunction in stress-related neuropsychiatric disorders (Courtney et al., 2013; Li and Sinha, 2008; Schwabe et al., 2013).

Declaration of conflicting interests

The authors declared that they had no conflicts of interest with respect to their research, authorship or the publication of this article.

Acknowledgements

We acknowledge Natural Scientific Foundation of China (No. 81771186) to RY and NIH grants AA021449, DA023248 and DA044749 to CRL for support of the study. The funders had no role in study design, data collection and analysis, decision to publish, or preparation of the manuscript.

References

Adler, S., Bicker, G., Bigalke, H., Bishop, C., Blumel, J., Dressler, D., Liebsch, M., 2010. The current scientific and legal status of alternative methods to the LD50 test for botulinum neurotoxin potency testing. The report and recommendations of a ZEBET Expert Meeting. Altern. Lab. Anim. 38 (4), 315–330.
Andreano, J.M., Arjomandi, H., Cahill, L., 2008. Menstrual cycle modulation of the relationship between cortisol and long-term memory. Psychoneuroendocrinology 33 (6), 874–882.
Aron, A.R., Behrens, T.E., Smith, S., Frank, M.J., Poldrack, R.A., 2007. Triangulating a cognitive control network using diffusion-weighted magnetic resonance imaging (MRI) and functional MRI. J. Neurosci. 27 (14), 3743–3752.
Aron, A.R., Poldrack, R.A., 2006. Cortical and subcortical contributions to stop signal response inhibition: role of the subthalamic nucleus. J. Neurosci. 26 (9), 2424–2433.
Ashburner, J., Friston, K.J., 1999. Nonlinear spatial normalization using basis functions. Hum. Brain Mapp. 7 (4), 254–266.
Büchel, C., Holmes, A., Rees, G., Friston, K., 1998. Characterizing stimulus–response functions using nonlinear regressors in parametric fMRI experiments. Neuroimage 8 (2), 140–148.
Bari, A., Robbins, T.W., 2013. Inhibition and impulsivity: behavioral and neural basis of response control. Prog. Neurobiol. 108, 44–79.
Chang, J., Yu, R., 2018a. Acute social stress modulates coherence regional homogeneity. Brain Imag. Behav. 1–9.
Chang, J., Yu, R., 2018b. Alternations in functional connectivity of amygdalar subregions under acute social stress. Neurobiol. Stress 9, 264–270.
Cohen, M.S., 1997. Parametric analysis of fMRI data using linear systems methods. Neuroimage 6 (2), 93–103.
Courtney, K.E., Ghahremani, D.G., Ray, L.A., 2013. Fronto-striatal functional connectivity during response inhibition in alcohol dependence. Addict. Biol. 18 (3), 593–604.
Della-Maggiore, V., Chau, W., Peres-Neto, P.R., McIntosh, A.R., 2002. An empirical comparison of SPM preprocessing parameters to the analysis of fMRI data. Neuroimage 17 (1), 19–28.
Deuschle, M., Schweiger, U., Weber, B., Gotthardt, U., Körner, A., Schmider, J., Heuser, I., 1997. Diurnal activity and pulsatility of the hypothalamus-pituitary-adrenal system in male depressed patients and healthy controls. J. Clin. Endocrinol. Metab. 82 (1), 234–238.
Diamond, A., 2013. Executive functions. Annu. Rev. Psychol. 64, 135–168.
Dierolf, A.M., Fechtner, J., Böhnke, R., Wolf, O.T., Naumann, E., 2017. Influence of acute stress on response inhibition in healthy men: an ERP study. Psychophysiology 54 (5), 684–695.
Dierolf, A.M., Schoofs, D., Hessas, E.-M., Falkenstein, M., Otto, T., Paul, M., Wolf, O.T., 2018. Good to be stressed? Improved response inhibition and error processing after acute stress in young and older men. Neuropsychologia 119, 434–447.
Duann, J.-R., Ide, J.S., Luo, X., Li, C.-s. R., 2009. Functional connectivity delineates distinct roles of the inferior frontal cortex and presupplementary motor area in stop signal inhibition. J. Neurosci. 29 (32), 10171–10179.
Duchesne, A., Pruessner, J.C., 2013. Association between subjective and cortisol stress response depends on the menstrual cycle phase. Psychoneuroendocrinology 38 (12), 3155–3159.
Farr, O.M., Hu, S., Zhang, S., Chiang-shan, R.L., 2012. Decreased saliency processing as a neural measure of Barratt impulsivity in healthy adults. Neuroimage 63 (3), 1070–1077.
Friston, K., Buechel, C., Fink, G., Morris, J., Rolls, E., Dolan, R., 1997. Psychophysiological and modulatory interactions in neuroimaging. Neuroimage 6 (3), 218–229.
Friston, K., Josephs, O., Zarahn, E., Holmes, A., Rouquette, S., Poline, J.-B., 2000. To smooth or not to smooth?: bias and efficiency in fmri time-series analysis. Neuroimage 12 (2), 196–208.
Friston, K.J., Harrison, L., Penny, W., 2003. Dynamic causal modelling. Neuroimage 19 (4), 1273–1302.
Friston, K.J., Holmes, A.P., Poline, J., Grasby, P., Williams, S., Frackowiak, R.S., Turner, R., 1995. Analysis of fMRI time-series revisited. Neuroimage 2 (1), 45–53.
Friston, K.J., Holmes, A.P., Worsley, K.J., Poline, J.P., Frith, C.D., Frackowiak, R.S., 1994. Statistical parametric maps in functional imaging: a general linear approach. Hum. Brain Mapp. 2 (4), 189–210.

Garrett, A.S., Maddock, R.J., 2001. Time course of the subjective emotional response to aversive pictures: relevance to fMRI studies. Psychiatry Res. Neuroimaging 108 (1), 39–48.
Ghahremani, D.G., Lee, B., Robertson, C.L., Tabibnia, G., Morgan, A.T., De Shetler, N., Mandelkern, M.A., 2012. Striatal dopamine D2/D3 receptors mediate response inhibition and related activity in frontostriatal neural circuitry in humans. J. Neurosci. 32 (21), 7316–7324.
Hu, J., Lee, D., Hu, S., Zhang, S., Chao, H., Li, C.S., 2016a. Individual variation in the neural processes of motor decisions in the stop signal task: the influence of novelty seeking and harm avoidance personality traits. Brain Struct. Funct. 221 (5), 2607–2618. https://doi.org/10.1007/s00429-015-1061-4.
Hu, S., Ide, J.S., Zhang, S., Sinha, R., Chiang-shan, R.L., 2015. Conflict anticipation in alcohol dependence—a model-based fMRI study of stop signal task. Neuroimage: Clinical 8, 39–50.
Hu, S., Li, C.S.R., 2012. Neural processes of preparatory control for stop signal inhibition. Hum. Brain Mapp. 33 (12), 2785–2796.
Hu, S., Zhang, S., Chao, H.H., Krystal, J.H., Li, C.S.R., 2016b. Association of drinking problems and duration of alcohol use to inhibitory control in nondependent young adult social drinkers. Alcohol Clin. Exp. Res. 40 (2), 319–328.
Jahfari, S., Waldorp, L., van den Wildenberg, W.P., Scholte, H.S., Ridderinkhof, K.R., Forstmann, B.U., 2011. Effective connectivity reveals important roles for both the hyperdirect (fronto-subthalamic) and the indirect (fronto-striatal-pallidal) fronto-basal ganglia pathways during response inhibition. J. Neurosci. 31 (18), 6891–6899.
Jiang, C., Rau, P.-L.P., 2017. The detrimental effect of acute stress on response inhibition when exposed to acute stress: an event-related potential analysis. Neuroreport 28 (14), 922–928.
Kirschbaum, C., Pirke, K.-M., Hellhammer, D.H., 1993. The 'trier social stress test' - a tool for investigating psychobiological stress responses in a laboratory setting. Neuropsychobiology 28, 76–81.
Krivoshapkin, V.G., Alexeev, V.P., Klimova, T.M., 2007. Cardiovascular diseases in the Republic of Sakha (Yakutia): status of the problem in the light of scientific research results. Alaska Med. 49 (2 Suppl. l), 48–50.
Kuhlmann, S., Wolf, O.T., 2005. Cortisol and memory retrieval in women: influence of menstrual cycle and oral contraceptives. Psychopharmacology (Berlin) 183 (1), 65–71.
Lawrence, A.J., Luty, J., Bogdan, N.A., Sahakian, B.J., Clark, L., 2009. Impulsivity and response inhibition in alcohol dependence and problem gambling. Psychopharmacology (Berlin) 207 (1), 163–172.
Levitt, H., 1971. Transformed up-down methods in psychoacoustics. J. Acoust. Soc. Am. 49 (2B), 467–477.
Li, C.-s. R., Huang, C., Constable, R.T., Sinha, R., 2006. Imaging response inhibition in a stop-signal task: neural correlates independent of signal monitoring and post-response processing. J. Neurosci. 26 (1), 186–192.
Li, C.-s. R., Huang, C., Yan, P., Paliwal, P., Constable, R.T., Sinha, R., 2008a. Neural correlates of post-error slowing during a stop signal task: a functional magnetic resonance imaging study. J. Cogn. Neurosci. 20 (6), 1021–1029.
Li, C.-s. R., Sinha, R., 2008. Inhibitory control and emotional stress regulation: neuroimaging evidence for frontal–limbic dysfunction in psycho-stimulant addiction. Neurosci. Biobehav. Rev. 32 (3), 581–597.
Li, C.-s. R., Yan, P., Sinha, R., Lee, T.-W., 2008b. Subcortical processes of motor response inhibition during a stop signal task. Neuroimage 41 (4), 1352–1363.
Li, C.s.R., Luo, X., Yan, P., Bergquist, K., Sinha, R., 2009. Altered impulse control in alcohol dependence: neural measures of stop signal performance. Alcohol Clin. Exp. Res. 33 (4), 740–750.
Liston, C., Miller, M.M., Goldwater, D.S., Radley, J.J., Rocher, A.B., Hof, P.R., McEwen, B.S., 2006. Stress-induced alterations in prefrontal cortical dendritic morphology predict selective impairments in perceptual attentional set-shifting. J. Neurosci. 26 (30), 7870–7874.
Logan, G.D., Cowan, W.B., Davis, K.A., 1984. On the ability to inhibit simple and choice reaction time responses: a model and a method. J. Exp. Psychol. Hum. Percept. Perform. 10 (2), 276.
Mani, A., Mullainathan, S., Shafir, E., Zhao, J., 2013. Poverty impedes cognitive function. Science 341 (6149), 976–980.
McEwen, B.S., Bowles, N.P., Gray, J.D., Hill, M.N., Hunter, R.G., Karatsoreos, I.N., Nasca, C., 2015. Mechanisms of stress in the brain. Nat. Neurosci. 18 (10), 1353–1363. https://doi.org/10.1038/nn.4086.
McGrath, E., Jones, A., Field, M., 2016. Acute stress increases ad-libitum alcohol consumption in heavy drinkers, but not through impaired inhibitory control. Psychopharmacology (Berlin) 233 (7), 1227–1234.
McRae, A.L., Saladin, M.E., Brady, K.T., Upadhyaya, H., Back, S.E., Timmerman, M.A., 2006. Stress reactivity: biological and subjective responses to the cold pressor and Trier Social stressors. Hum. Psychopharmacol. Clin. Exp. 21 (6), 377–385.
Mika, A., Mazur, G.J., Hoffman, A.N., Talboom, J.S., Bimonte-Nelson, H.A., Sanabria, F., Conrad, C.D., 2012. Chronic stress impairs prefrontal cortex-dependent response inhibition and spatial working memory. Behav. Neurosci. 126 (5), 605.
Mizoguchi, K., Yuzurihara, M., Ishige, A., Sasaki, H., Chui, D.-H., Tabira, T., 2000. Chronic stress induces impairment of spatial working memory because of prefrontal dopaminergic dysfunction. J. Neurosci. 20 (4), 1568–1574.
Morein-Zamir, S., Robbins, T.W., 2015. Fronto-striatal circuits in response-inhibition: relevance to addiction. Brain Res. 1628, 117–129.
Mueller, S.C., Maheu, F.S., Dozier, M., Peloso, E., Mandell, D., Leibenluft, E., Ernst, M., 2010. Early-life stress is associated with impairment in cognitive control in adolescence: an fMRI study. Neuropsychologia 48 (10), 3037–3044.
Nicholson, A.A., Rabellino, D., Densmore, M., Frewen, P.A., Paret, C., Kluetsch, R., McKinnon, M.C., 2017. The neurobiology of emotion regulation in posttraumatic stress disorder: amygdala downregulation via real-time fMRI neurofeedback. Hum. Brain Mapp. 38 (1), 541–560.
Passamonti, L., Rowe, J.B., Ewbank, M., Hampshire, A., Keane, J., Calder, A.J., 2008. Connectivity from the ventral anterior cingulate to the amygdala is modulated by appetitive motivation in response to facial signals of aggression. Neuroimage 43 (3), 562–570.
Passamonti, L., Rowe, J.B., Schwarzbauer, C., Ewbank, M.P., Von Dem Hagen, E., Calder, A.J., 2009. Personality predicts the brain's response to viewing appetizing foods: the neural basis of a risk factor for overeating. J. Neurosci. 29 (1), 43–51.
Penny, W.D., Stephan, K.E., Daunizeau, J., Rosa, M.J., Friston, K.J., Schofield, T.M., Leff, A.P., 2010. Comparing families of dynamic causal models. PLoS Comput. Biol. 6 (3), e1000709.
Penny, W.D., Stephan, K.E., Mechelli, A., Friston, K.J., 2004. Comparing dynamic causal models. Neuroimage 22 (3), 1157–1172.
Qi, M., Gao, H., Liu, G., 2017. Effect of acute psychological stress on response inhibition: an event-related potential study. Behav. Brain Res. 323, 32–37.
Qin, S., Hermans, E.J., van Marle, H.J., Fernández, G., 2012. Understanding low reliability of memories for neutral information encoded under stress: alterations in memory-related activation in the hippocampus and midbrain. J. Neurosci. 32 (12), 4032–4041.
Quirarte, G.L., De La Teja, I.S.L., Casillas, M., Serafín, N., Prado-Alcalá, R.A., Roozendaal, B., 2009. Corticosterone infused into the dorsal striatum selectively enhances memory consolidation of cued water-maze training. Learn. Mem. 16 (10), 586–589.
Rand, D.G., Greene, J.D., Nowak, M.A., 2012. Spontaneous giving and calculated greed. Nature 489 (7416), 427.
Roos, L.E., Knight, E.L., Beauchamp, K.G., Berkman, E.T., Faraday, K., Hyslop, K., Fisher, P.A., 2017. Acute stress impairs inhibitory control based on individual differences in parasympathetic nervous system activity. Biol. Psychol. 125, 58–63.
Schlosser, N., Wolf, O.T., Fernando, S.C., Terfehr, K., Otte, C., Spitzer, C., Wingenfeld, K., 2013. Effects of acute cortisol administration on response inhibition in patients with major depression and healthy controls. Psychiatry Res. 209 (3), 439–446.
Schmidt, A., Palaniyappan, L., Smieskova, R., Simon, A., Riecher-Rössler, A., Lang, U.E., Borgwardt, S.J., 2016. Dysfunctional insular connectivity during reward prediction in patients with first-episode psychosis. J. Psychiatry Neurosci.: JPN 41 (6), 367.
Scholz, U., La Marca, R., Nater, U.M., Aberle, I., Ehlert, U., Hornung, R., Kliegel, M., 2009. Go no-go performance under psychosocial stress: beneficial effects of implementation intentions. Neurobiol. Learn. Mem. 91 (1), 89–92.
Schwabe, L., 2013. Stress and the engagement of multiple memory systems: integration of animal and human studies. Hippocampus 23 (11), 1035–1043. https://doi.org/10.1002/hipo.22175.
Schwabe, L., Höffken, O., Tegenthoff, M., Wolf, O.T., 2013. Stress-induced enhancement of response inhibition depends on mineralocorticoid receptor activation. Psychoneuroendocrinology 38 (10), 2319–2326.
Schwabe, L., Haddad, L., Schachinger, H., 2008. HPA axis activation by a socially evaluated cold-pressor test. Psychoneuroendocrinology 33 (6), 890–895.
Schwabe, L., Tegenthoff, M., Hoffken, O., Wolf, O.T., 2012. Simultaneous glucocorticoid and noradrenergic activity disrupts the neural basis of goal-directed action in the human brain. J. Neurosci. 32 (30), 10146–10155. https://doi.org/10.1523/jneurosci.1304-12.2012.
Schwabe, L., Wolf, O.T., 2011. Stress-induced modulation of instrumental behavior: from goal-directed to habitual control of action. Behav. Brain Res. 219 (2), 321–328.
Schwabe, L., Wolf, O.T., 2012. Stress modulates the engagement of multiple memory systems in classification learning. J. Neurosci. 32 (32), 11042–11049. https://doi.org/10.1523/jneurosci.1484-12.2012.
Seghier, M.L., Price, C.J., 2009. Reading aloud boosts connectivity through the putamen. Cerebr. Cortex 20 (3), 570–582.
Seghier, M.L., Zeidman, P., Neufeld, N.H., Leff, A.P., Price, C., 2010. Identifying abnormal connectivity in patients using Dynamic Causal Modelling of fMRI responses. Front. Syst. Neurosci. 4, 142.
Sharp, D., Bonnelle, V., De Boissezon, X., Beckmann, C., James, S., Patel, M., Mehta, M.A., 2010. Distinct frontal systems for response inhibition, attentional capture, and error processing. Proc. Natl. Acad. Sci. 107 (13), 6106–6111.
Shields, G.S., Bonner, J.C., Moons, W.G., 2015. Does cortisol influence core executive functions? A meta-analysis of acute cortisol administration effects on working memory, inhibition, and set-shifting. Psychoneuroendocrinology 58, 91–103.
Shields, G.S., Sazma, M.A., Yonelinas, A.P., 2016a. The effects of acute stress on core executive functions: a meta-analysis and comparison with cortisol. Neurosci. Biobehav. Rev. 68, 651–668.
Shields, G.S., Trainor, B.C., Lam, J.C., Yonelinas, A.P., 2016b. Acute stress impairs cognitive flexibility in men, not women. Stress 19 (5), 542–546.
Simmonds, D.J., Pekar, J.J., Mostofsky, S.H., 2008. Meta-analysis of Go/No-go tasks demonstrating that fMRI activation associated with response inhibition is task-dependent. Neuropsychologia 46 (1), 224–232.
Starcke, K., Wiesen, C., Trotzke, P., Brand, M., 2016. Effects of acute laboratory stress on executive functions. Front. Psychol. 7, 461.
Stephan, K.E., Penny, W.D., Daunizeau, J., Moran, R.J., Friston, K.J., 2009. Bayesian model selection for group studies. Neuroimage 46 (4), 1004–1017.
Steptoe, A., Hamer, M., Chida, Y., 2007. The effects of acute psychological stress on circulating inflammatory factors in humans: a review and meta-analysis. Brain Behav. Immun. 21 (7), 901–912.
Swann, N.C., Cai, W., Conner, C.R., Pieters, T.A., Claffey, M.P., George, J.S., Tandon, N., 2012. Roles for the pre-supplementary motor area and the right inferior frontal gyrus in stopping action: electrophysiological responses and functional and structural connectivity. Neuroimage 59 (3), 2860–2870.

Takahashi, T., Ikeda, K., Hasegawa, T., 2007. Social evaluation-induced amylase elevation and economic decision-making in the dictator game in humans. Neuroendocrinol. Lett. 28 (5), 662–665.

Tzourio-Mazoyer, N., Hervé, P.Y., Mazoyer, B., 2007. Neuroanatomy: tool for functional localization, key to brain organization. Neuroimage 37 (4), 1059–1060. https://doi.org/10.1016/j.neuroimage.2007.02.007.

Ulrich-Lai, Y.M., Herman, J.P., 2009. Neural regulation of endocrine and autonomic stress responses. Nat. Rev. Neurosci. 10 (6), 397–409.

van Marle, H.J.F., Hermans, E.J., Qin, S., Fernández, G., 2010. Enhanced resting-state connectivity of amygdala in the immediate aftermath of acute psychological stress. Neuroimage 53 (1), 348–354. https://doi.org/10.1016/j.neuroimage.2010.05.070.

Verbruggen, F., Logan, G.D., 2008. Response inhibition in the stop-signal paradigm. Trends Cogn. Sci. 12 (11), 418–424.

Von Dawans, B., Fischbacher, U., Kirschbaum, C., Fehr, E., Heinrichs, M., 2012. The social dimension of stress reactivity: acute stress increases prosocial behavior in humans. Psychol. Sci. 23 (6), 651–660.

Watson, D., Clark, L.A., Tellegen, A., 1988. Development and validation of brief measures of positive and negative affect: the PANAS scales. J. Personal. Soc. Psychol. 54 (6), 1063.

Wellman, C.L., 2001. Dendritic reorganization in pyramidal neurons in medial prefrontal cortex after chronic corticosterone administration. Dev. Neurobiol. 49 (3), 245–253.

Wetherill, G., Chen, H., Vasudeva, R., 1966. Sequential estimation of quantal response curves: a new method of estimation. Biometrika 53 (3–4), 439–454.

Yu, R., 2016. Stress potentiates decision biases: a stress induced deliberation-to-intuition (SIDI) model. Neurobiol. Stress 3, 83–95. https://doi.org/10.1016/j.ynstr.2015.12.006.

Zandbelt, B.B., Vink, M., 2010. On the role of the striatum in response inhibition. PLoS One 5 (11), e13848.

Zheng, D., Oka, T., Bokura, H., Yamaguchi, S., 2008. The key locus of common response inhibition network for no-go and stop signals. J. Cogn. Neurosci. 20 (8), 1434–1442.